

# Drag reduction on a circular cylinder by corona discharge

Renev M.E., Safronova I.F.  
m.renev@2014.spbu.ru

## Abstract

The paper considers the capability of ion wind, caused by corona discharge, of changing the wake structure behind a circular cylinder, the maximum Reynolds number being 3600. Computer simulation of positive corona discharge uses the unipolar model. The electrode system consists of a grounded circular cylinder and a high-voltage wire placed behind the cylinder. The corona discharge has been shown to be capable of changing the wake structure of Karman vortex street significantly. Frequencies of the vortices decrease 2.5 times with applications of 30 kV voltage, sizes and rotation speeds of the vortices increasing notably as well. The drag force is mostly defined by the pressure distribution on the cylinder surface and displays quasi-periodic behavior. The average value of the force is a linear function for studied voltages. The value decreases markedly with increasing voltage.

## 1 Introduction

The control of aerodynamic characteristics of bodies is an important applied problem of mechanics. When a body is bluff, the viscosity component of the drag force is less than pressure one, so the problem of lowering the drag force in the case reduces to that of making the pressure difference on the surface of the bluff body smaller. The pressure drag force emerges because of the boundary layer separation. There are many ways of changing the separation angle, both active and passive. The former require additional power and include blowing out the separated layer, acoustic perturbation, vibrating walls. The latter comprise regulating surface roughness and placing wake structure separators. When the Reynolds number is  $50\text{-}10^5$ , the Karman vortex street behind bluff bodies appears [1]. It is a periodic motion with vortices, which detach alternately from the top and the bottom of the body. Mechanical oscillations, caused by vortices, might bring about vibrations, noise and even the system destruction.

Despite many studies in the field of physics, of interest today is controlling the wake structures by ion wind, caused by a corona discharge. The manner of control has many advantages: it is simple, robust, cost-effective, and has no moving parts.

A corona discharge occurs in electrode systems with small curvature radius; this is needed to establish strong and localized electric field near the sharp electrode. The

field makes charged particles collide and thus ionize, so the number of ions in the air grows exponentially. The region, where the electric field is strong enough to ensure the collisions, is called the corona sheath and is typically rather small (near 0.1 mm in radius). Outside the corona sheath, the ions drift under the action of the electric field and share their momenta with neutral particles in collisions; the air is set in motion in the direction from the sharp electrode to the grounded one. This phenomenon is called the ion wind.

The paper presents the computer simulation of the positive corona discharge and the ion wind. In case of the positive corona discharge, electrons appear near corona sheath because of photoionization [2], are drawn into the sheath, forming an avalanche, and disappear on the surface of the sharp electrode. The flux of the positive ions moves outwards. The simulation uses an original unipolar model of the positive corona discharge, which replaces the ionization processes in the sheath with a boundary condition on the sharp electrode [3, 6]. The input parameters include physical quantities, which can be measured independent, such as ionization rate, ions mobility, diffusion coefficient, critical value of ionization collisions. The authors of the current paper sought to demonstrate the capability of controlling the wake structures of the airflow near a circular cylinder by means of a corona discharge. The drag force was calculated, the Karman vortex street was analyzed in great detail, and it was shown how these characteristics change when a voltage is applied.

## 2 Simulation

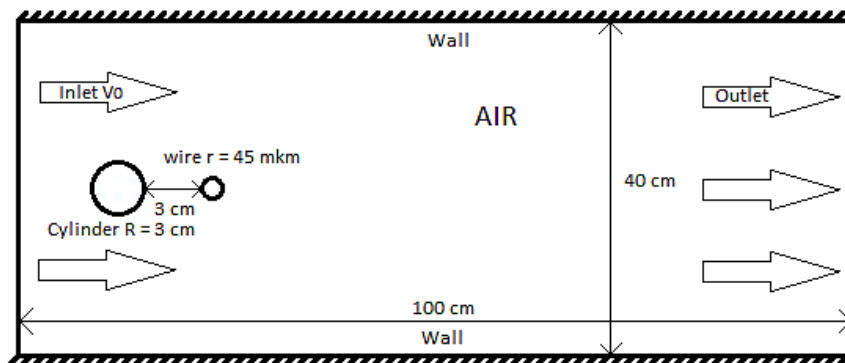


Figure 1: Geometry for the computer simulation (wire is not in scale).

The wire-cylinder electrode system is placed into an aerodynamic tunnel with airflow velocity  $V_0$ . The wire has radius  $r = 45 \mu\text{m}$  and is at a high voltage, the cylinder has a radius  $R = 3 \text{ cm}$  and is grounded. The wire is placed behind the cylinder, and the electrodes are spaced at 3 cm. Figure 1 shows the geometry of computer model. Simulation used the plane geometry with width  $L = 28 \text{ cm}$ . Inflow velocities  $V_0$  were 0.6 m/s and 0.8 m/s; the Reynolds numbers for the velocities in case of the circular cylinder and no applied pressure are 2700 and 3600, respectively. The applied voltage was in range 16.2kV-30kV. The experiments [4] show that, when the

voltage is more than 30 kV, an electric breakdown occurs in such electrode systems.

$$\Delta\varphi = -\frac{|e|n_+}{\varepsilon_0} \quad (1)$$

$$\vec{E} = -\nabla\varphi \quad (2)$$

$$\frac{\partial n_+}{\partial t} + \text{div} \left[ -D\nabla n_+ + bn_+ \vec{E} \right] = 0 \quad (3)$$

$$\rho \frac{d\vec{v}}{dt} = -\nabla p + \eta \Delta \vec{v} + |e|n_+ \vec{E} \quad (4)$$

$$\text{div} \vec{v} = 0 \quad (5)$$

$$\frac{\partial j_s}{\partial t} = j_s \frac{e^{-M_{cr}} e^M - 1}{\tau} \quad (6)$$

$$M = \int_0^s \alpha_{eff}(E(s)) ds \quad (7)$$

The mathematical model of ion wind includes Poisson equation (1) for the electric potential  $\varphi$ , the equation linking the electric field  $\vec{E}$  and the potential (2), the Nernst-Boltzmann equation (3) for the concentration of positive ions  $n_+$ , the Navier-Stokes equation for the air velocity  $\vec{v}$  and the pressure  $p$  (4) with external volume force, the continuity equation (5) for incompressible air. The unipolar model [3, 6] includes boundary condition (6) for the partial time derivative of positive ions flux density  $j_s$  from the sheath of corona discharge to exterior. The  $e^{-M_{cr}}$  coefficient is an photoionization coefficient,  $M$  is the collision number (7) along the electric field line in the corona sheath, which depends on effective ionization coefficient  $\alpha_{eff}$ ,  $s$  is the coordinate along the electric field line,  $\tau = 10^{-3}$ s is the characteristic time.  $M_{cr}$  is the value of ionization collisions needed for the discharge ignition. Boundary conditions are shown in the table 18 ( $\vec{n}$  is the normal vector of surface,  $\vec{e}_x$  is the x-axis vector,  $U$  is the applied voltage).

Table 18: Boundary conditions for the simulation

	air flow	electrostatics	transporting of ions
wall	$\vec{v} = \vec{0}$	$\vec{n} * \vec{E} = 0$	$\vec{n} * (-D\nabla n_+ - bn_+ \vec{E}) = 0$
inlet	$\vec{v} = V_0 * \vec{e}_x$	$\vec{n} * \vec{E} = 0$	$\vec{n} * (-D\nabla n_+ - bn_+ \vec{E}) = 0$
outlet	$\sum_{j=1}^3 [-p\delta_{ij} + \eta\sigma_{ij}] n_j = -p^* n_i; p^* \leq 0$ $\sigma_{ij} = \frac{\partial v_i}{\partial x_j} + \frac{\partial v_j}{\partial x_i}$ (zero relative pressure)	$\vec{n} * \vec{E} = 0$	$\vec{n} * (-D\nabla n_+ - bn_+ \vec{E}) = 0$
wire	$\vec{v} = \vec{0}$	$\varphi = U$	$j_s$ (5)
cylinder	$\vec{v} = \vec{0}$	$\varphi = 0$	$j_\tau = 0$

$\eta$  is the air viscosity ( $16 \mu\text{Pa}\cdot\text{s}$ ),  $\rho$  is the air density ( $1.2 \text{ kg}/\text{m}^3$ ),  $e$  is the electron charge ( $1.6 \cdot 10^{-19} \text{ C}$ ),  $D$  is the effective diffusion coefficient of positive ions ( $10 \text{ mm}^2/\text{s}$ ),  $b$  is the effective mobility of positive ions ( $2.14 \cdot 10^{-4} \text{ m}^2/(\text{V}\cdot\text{s})$ ),  $\varepsilon_0$  is the vacuum dielectric permittivity ( $8.85 \cdot 10^{-12} \text{ F}/\text{m}$ ). The simulation was carried out with COMSOL Multiphysics.

### 3 Results

The calculated current-voltage curve (I-V curve) of the corona discharge agrees quite well with the experimental one [4] for given electrode system Figure ???. The I-V curve is the quadratic function and equation (??) is suitable for it:

$$I = KU(U - U_0) \tag{8}$$

K - is the coefficient of I-V curve growth and depends on geometry of electrodes and the positive ion mobility. b was taken equal  $2.1 \cdot 10^{-4} \text{ m}^2/(\text{V} \cdot \text{s})$ , it conform with data from different literature [2, 5].  $U_0$  - is the treshold voltage, which depends on  $M_{cr}$ . For this study  $M_{cr} = 11$ , so treshold voltage is nearly 7 kV. This value of  $M_{cr}$  also was used in studies [3, 5] and match with experiments. Figure (??) shows, that the experimental treshold voltage is nearly 10 kV. If  $M_{cr}$  increases, the treshold voltage does so, too. The treshold voltages may be made equal, but  $M_{cr} = 18-20$  is the value of streamer ignition. Such difference between current at low voltages less than 10 kV might be caused by currents too low for registration.

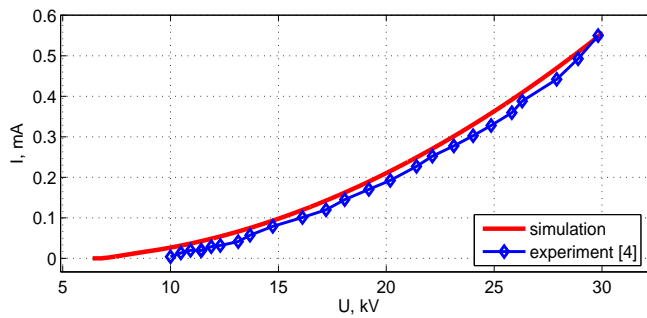


Figure 2: The I-V curve of the corona discharge: the simulation and the experiment [4].

When  $U$  and  $V_0$  attain steady-state, the airflow is considered quasi-periodic. Figure ??a shows Karman vortex street without the corona discharge at  $V_0 = 0.6 \text{ m/s}$ , and Figure ??b shows the street with the applied voltage 21.2 kV at  $V_0 = 0.6 \text{ m/s}$ . The ion wind moves from the wire to the cylinder and it pushes vortexes to the cylinder and enhance them. This phenomenon could be called "ion wind enhancement of vortexes". Figure ??b shows the vortexes that much bigger than common ones. The maximal vortex radius in this paper is nearly 2 times bigger than the cylinder radius and the maximal rotation speed increases in 3 times.

In addition, there is a region between the vortex and the cylinder, where small vortices may occur and cause small and fast oscillations of the drag force (Figure 4).

Figure 4 shows the time-dependent drag force  $F(t)$  at  $V_0 = 0.6 \text{ m/s}$  and  $U = 0 \text{ kV}$ ; 21.2 kV. There are quasi-periodic oscillations. If a voltage is applied, the main period becomes longer, the amplitude rises, the mean value decreases. The shape of oscillations becomes non-harmonic.

Figure 5 shows one period of the drag force for some parameters  $V_0, U$ . The part, where  $F(t)$  is decreasing, is considered the part of the vortex accumulation, the

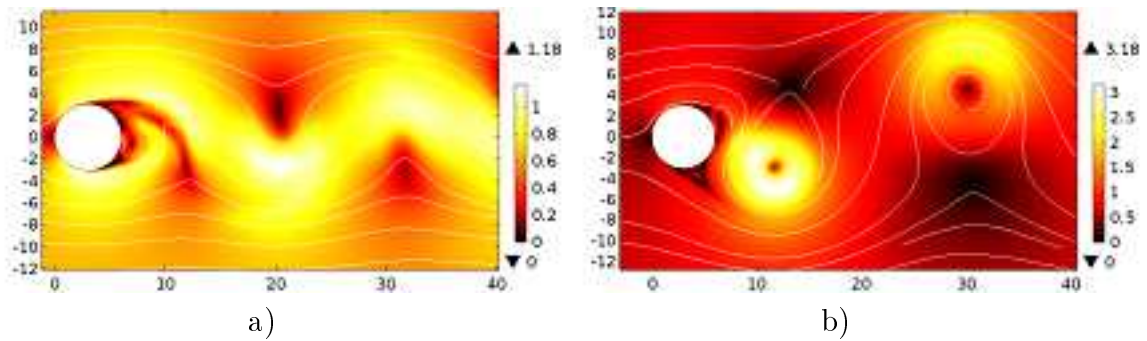


Figure 3: Contour plots of air velocity with streamlines. 3a:  $V_0 = 0.6$  m/s  $U = 0$  kV; 3b:  $V_0 = 0.6$  m/s,  $U = 21.2$  kV.

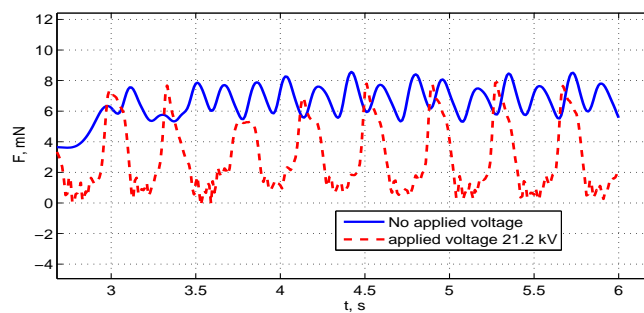


Figure 4: The drag force vs. time for cases: no applied voltage and  $U = 21.2$  kV;  $V_0 = 0.6$  m/s.

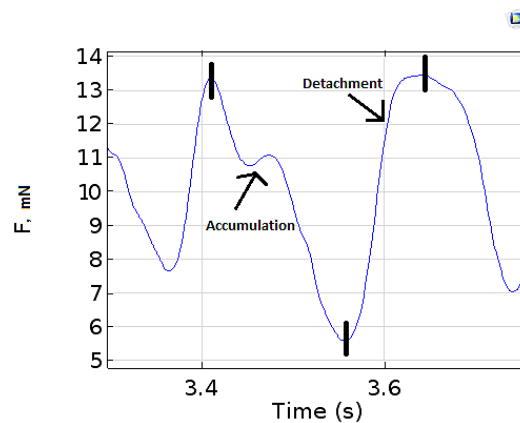


Figure 5: The accumulation and the detachment parts of a period of drag force.

second part is the vortex detachment. While the voltage is increasing, the accumulation part becomes longer. So, it has to be considered that the vortices plays the main role in the drag reduction. If the accumulation time grows, the mean value of the drag force decreases. Below, some relative dimensionless quantities will be calculated. The equation for them is number (9): a ratio of the value of a quantity at some applied voltage to its value without applied voltage.

$$\text{relative variable} = \frac{\text{variable}(U)}{\text{variable}(U = 0)} \quad (9)$$

Figure 6 shows the relative variable of the vortex frequencies.  $\text{Freq}(U = 0, V_0 = 0.8 \text{ m/s}) = 8.13 \text{ Hz}$ ,  $\text{Freq}(U = 0, V_0 = 0.6 \text{ m/s}) = 5.48 \text{ Hz}$ .

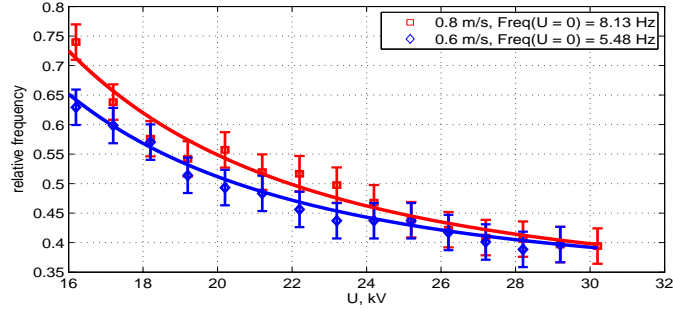


Figure 6: Relative frequency of vortexes vs applied voltage for different velocities of inflow.

As it was expected, when  $V_0$  rises, the frequency rises, too, because higher velocities make vortices move away faster. At  $U = 30 \text{ kV}$ , the relative frequency decreased 2.5 times. It happens because of the stronger ion wind push on vortices; the accumulation time and sizes of vortices increase.

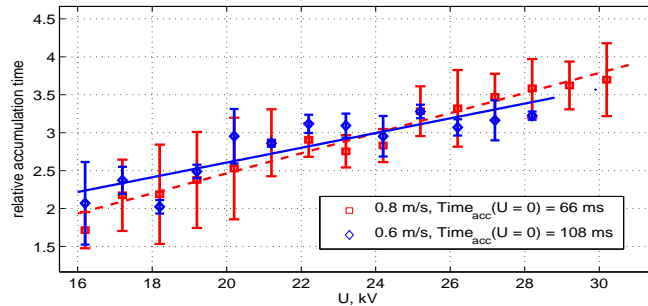


Figure 7: The accumulation time vs applied voltage for different inflow velocities.

Figure 7 shows dependence between the relative accumulation time and the applied voltage for different inflow velocities.  $\text{Time}_{acc}(U = 0, V_0 = 0.8 \text{ m/s}) = 66 \text{ ms}$ ,  $\text{Time}_{acc}(U = 0, V_0 = 0.6 \text{ m/s}) = 108 \text{ ms}$ . The accumulation time rises along with the voltage. In addition, the time plays the main role in the frequency decreasing. Figure 8 shows the relative detachment angle vs applied voltage at different inflow velocities. The angles are reckoned counter-clockwise and the starting point is the most right point of the cylinder (Figure 1). There are voltages, where angles are nearly constant. Afterwards, the visible rise occurs, which starts earlier at smaller inflow velocities. It is related with the phenomenon of the wind enhancement of vortices. The enhanced vortices significantly change the wake structure and might be considered as obstacles so the angle increases. The plot can be used to evaluate the voltage, at which small oscillations of the drag force occur.

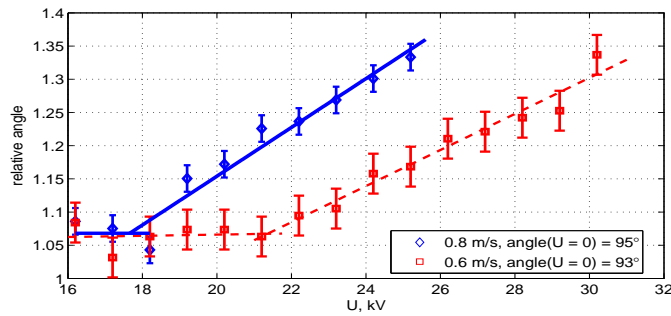


Figure 8: The relative detachment angle vs the applied voltage for different inflow velocities.

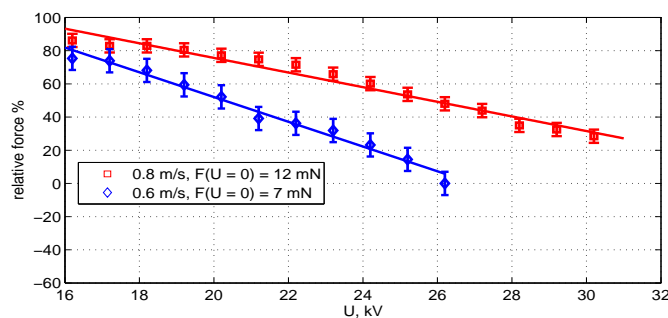


Figure 9: The relative mean value of drag force vs. the applied voltage for different inflow velocities.

Figure 9 shows the relative mean value of drag force vs. the applied voltage at different inflow velocities. The mean value is a decreasing linear function of the applied voltage. For higher inflow velocities, the mean value decreases slower. For  $V_0=0.6$  m/s,  $U = 26$  kV is the voltage, at which the drag force is zero. At this voltage, the ion wind effect balances the one of the external flow.

## 4 Conclusion

The simulation has shown the corona discharge to significantly change the periodic behavior of Karman vortex street. The maximal drop of the vortex frequencies is 2.5 for  $U = 30$  kV as compared with  $U = 0$  kV. At high voltages, the vortices can accumulate more momentum, because the corona discharge pushes them stronger. Increasing the accumulation time by corona discharge can reduce the mean value of the drag force. The pressure distribution plays a major part in the drag force. The mean value of drag force is a linear function of the applied voltage. The drag force is quasi-periodical. There is a voltage, at which the drag force is zero. For higher velocities, all considered effects are less noticeable, because the vortices move away faster.

## 5 Acknowledgements

Research was carried out using computer resources provided by Resource Center "Computer Center of SPbU" (<http://cc.spbu.ru>).

## References

- [1] Milton van Dyke. An album of fluid motion. Parabolic Press, 1982, 176 p.
- [2] Yu. P. Raizer. Gas Discharge Physics. Springer, Berlin, New York, 1991, 450 p.
- [3] A.V. Samusenko, I.F. Safronova, Yu.K. Stishkov. Unipolar model of the positive corona discharge. Surface Engineering and Applied Electrochemistry, 2016, 52(5), pp.43-БГҮ50.(in russian)
- [4] K.T. Hyun, C.H. Chun. The wake flow control behind a circular cylinder using ion wind. Experiments in Fluids, 2003, 35, pp. 541–552 DOI 10.1007/s00348-003-0668-z.
- [5] Yu. K. Stishkov, A.V. Samusenko. Electrophysical processes in gases in strong electric field. 2011, 567 p.
- [6] P. S. Zhidkova, A. V. Samusenko. A computer model of the ionic wind in the unipolar approximation with the boundary condition on the ion flow variation rate. Surface Engineering and Applied Electrochemistry, 2016, 52(4), pp. 370-БГҮ379. doi: 10.3103/S106837551604013X.

*Renev M. E., Safronova I. F, St. Petersburg State University 7/9 Universitetskaya nab., St. Petersburg, 199034 Russia.*